

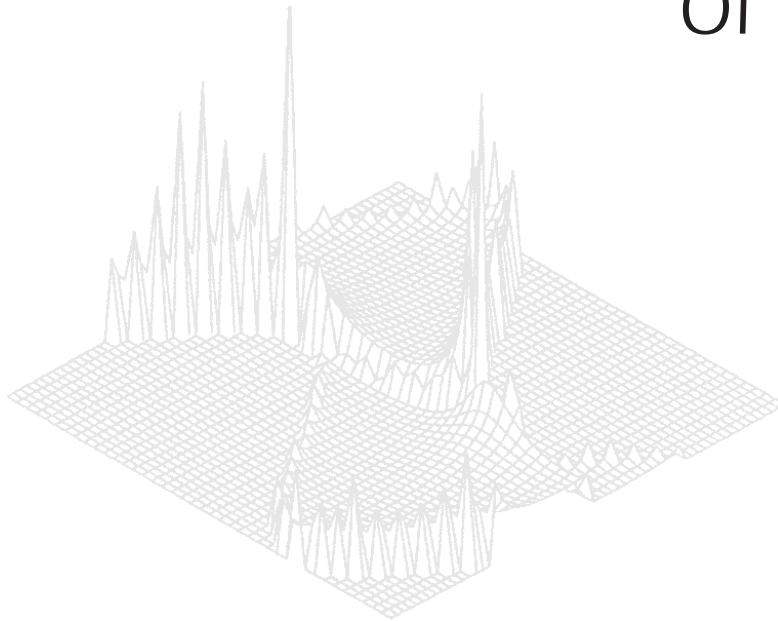
---

**C S I R O   P U B L I S H I N G**

---

# Australian Journal of Physics

Volume 51, 1998  
© CSIRO 1998



A journal for the publication of  
original research in all branches of physics

**[www.publish.csiro.au/journals/ajp](http://www.publish.csiro.au/journals/ajp)**

All enquiries and manuscripts should be directed to  
*Australian Journal of Physics*

**CSIRO PUBLISHING**

PO Box 1139 (150 Oxford St)

Collingwood

Vic. 3066

Australia

Telephone: 61 3 9662 7626

Facsimile: 61 3 9662 7611

Email: [peter.robertson@publish.csiro.au](mailto:peter.robertson@publish.csiro.au)



Published by **CSIRO PUBLISHING**  
for CSIRO and the  
Australian Academy of Science



## Nuclear Spin-lattice Relaxation Rates of Ni and Ru in Fe\*

*E. Beck, W. D. Brewer, T. Funk and E. Klein*

Fachbereich Physik, Freie Universität Berlin,  
14195 Berlin, Germany.

### *Abstract*

We have determined the nuclear spin-lattice relaxation (SLR) rates of Ni and Ru as dilute impurities in iron using the method of thermal cycling on oriented nuclei. The samples were prepared by recoil implantation from the heavy ion reactions used to produce the radioactive Ni and Ru isotopes employed in the measurements. In the 3d impurity series, only Sc, Ti, and Cu remain to complete the systematics of the SLR in iron host; in the 4d series, values for Zr and Pd are still missing and the datum for Rh has a large experimental uncertainty. We discuss the comparison with theory and with other experimental results.

### 1. Introduction

The nuclear spin-lattice relaxation (SLR) rate of impurity nuclei in solids reflects the *dynamic* hyperfine interaction and provides an interesting complement to static quantities (magnetic hyperfine fields, electric quadrupole field gradients, isomer shifts). A number of dilute impurities in Fe host have been studied by hyperfine methods in the past, but usually with emphasis on the determination of static quantities, so that the SLR rates were not measured precisely, if at all. More than 20 years ago, a systematic study of *nd* series impurities in Fe using spin-echo resonance was carried out by Masuda *et al.* (1974); however, several gaps remained where no suitable NMR nucleus was available. Furthermore, for sensitivity reasons the experiments were performed mainly on powder samples with relatively high impurity concentrations (typically more than 1 at.%). This is problematic especially for the heavier impurity elements owing to their limited solubilities and the possibility of unresolved quadrupole splittings in the broad resonance lines.

Our group has for some years carried out a program of systematic investigation of the SLR rates of *nd* impurities in Fe and other host metals using the method of thermal cycling of oriented nuclei (TCON; see Klein 1986). This method, based on the use of thermal-equilibrium initial and final states for the relaxation, avoids the questions raised by resonant methods where the initial-state preparation is less well-defined. It is also practically independent of the applied magnetic field,

\* Refereed paper based on a contribution to the International Workshop on Nuclear Methods in Magnetism, held in Canberra on 21–22 July 1997.

allowing in many cases detailed studies of the field dependence of the SLR rates. Its principal drawback lies in its being an integral method, so that the origin of the observed anisotropy of nuclear radiations must be established by careful sample preparation and determination of the temperature dependence of the anisotropy prior to beginning a TCON measurement. However, we note that the presence of a non-orienting component of the radiation has essentially no effect on the results of the SLR measurement.

Field dependence studies have shown that for most impurities in Fe, a notable increase in SLR rate occurs with decreasing applied magnetic field below about 1 T, leading to a factor of 2 or more increased rate near zero applied fields. This field dependence is not simply related to the magnetisation curve of the host material, but is usually well described as the sum of a high-field or *intrinsic rate*  $r_\infty$  and an additional rate  $r(B)$  which is proportional to the square of the ferromagnetic enhancement factor  $\eta$ , familiar from NMR in ferromagnets. This experimental fact, which as yet has no solid theoretical basis, is referred to as the *enhancement-factor model* (EFM). Neglecting this field dependence has often led to erroneous or misleading values of the SLR rates in the literature, since only the intrinsic rate  $r_\infty$  can be directly compared with theoretical predictions or even with experiments on other samples of the same impurity/host element combination.

Attempting to explain their spin-echo data, Masuda *et al.* (1974) developed a phenomenological model which included the spin and orbital contributions of *s*, *p* and *d* electrons and also the Weger (1962) mechanism, based on the excitation and absorption of virtual spin-waves by the relaxing nuclei (VSW mechanism). The resulting calculated SLR rates overestimated even many of their own experimental values, which have since been found to be systematically too high, probably for the reasons mentioned above. Much later, Akai and others (1988, 1990) used the KKR–Green Function method to perform the first *ab initio* calculations of SLR rates for nearly all elements as impurities in Fe. His calculated rates reproduce well the general trends in  $r_\infty$  as a function of impurity  $Z$ , but are systematically too low in magnitude. This quantitative discrepancy is important for the light-element impurities ( $Z < 20$ ), then becomes smaller (less than ca. 50% underestimation of the rates) for the 3d series, increasing to ca. 100% in the 4d series, and is again quite large (a factor of 3 or more) in the 5d series (cf. the companion paper on the SLR rates of 5d series impurities in Fe, Beck *et al.* 1998a, present issue p. 281). A possible explanation, suggested by Akai, is the neglect in the calculations of lattice relaxation around the impurities due to size mismatch with the host lattice; for the Fe host, this is clearly most serious for the light elements and for the heavy 5d elements. Calculations for a few selected cases including lattice relaxation might clarify this point. One of us (E.K.) has also suggested that taking into consideration the VSW mechanism might greatly improve the agreement between experiment and theory (cf. Bobek *et al.* 1993). The *ab initio* theory cannot at present include this mechanism, which involves host spin dynamics, but the phenomenological estimate of Masuda *et al.* (1974) can simply be added to the rates calculated by the *ab initio* theory, and the result does indeed greatly improve the quantitative agreement with experiment where reliable data are available (cf. also Beck *et al.* 1998a). Additional support for the possible importance of the VSW mechanism comes from the Munich

group (Seewald *et al.* 1997), who have recently found evidence that spin-wave processes can explain the field dependence of the SLR rate in a particular case, and thus may perhaps play a role in the intrinsic rates as well.

Here, we present new determinations of  $r_\infty$  for two elements in the 3d and 4d series as impurities in Fe:  $^{57}\text{NiFe}$  and  $^{97}\text{RuFe}$ . Both represent maxima in the theoretical relaxation rate systematics, but were experimentally unknown or uncertain up to now. The case of Ni impurities is particularly intractable, since the sole NMR isotope of this element has only ca. 1% natural abundance and is thus difficult to study; other methods, such as PAC, PAD or nuclear orientation, are also not readily applicable. The only isotope suitable for nuclear orientation or NMR/ON studies is 1.5 d  $^{57}\text{Ni}$ ; however, its  $\gamma$  rays have very unfavourable branching ratios and anisotropy coefficients and, as an impurity in Fe, it has a low interaction temperature ( $T_{\text{int}} = B_{\text{eff}}\mu\mu_{\text{N}}/Ik$ ) of 4.5 mK, requiring rather low temperatures for a sensitive experiment. An early study (Rosenblum and Steyert 1975) used its  $\gamma$ -ray anisotropy at very low temperatures to measure the nuclear moment of the  $I = \frac{3}{2}$  parent state, but the accuracy was limited. Recently, Ohtsubo *et al.* (1996) detected the  $\beta$  particles from  $^{57}\text{Ni}$  oriented in Fe and used their asymmetry to carry out NMR/ON. They also used the FM-on/off method to observe the SLR of  $\text{NiFe}$ .

The second case studied in this work is  $^{97}\text{RuFe}$ . There are in principle two NMR isotopes of Ru and several isotopes suitable for other hyperfine techniques; however, only a few experiments on  $\text{RuFe}$  have been reported. Ruthenium is isoelectronic to Fe and its SLR rate is predicted to show a strong maximum within the 4d series. An early NMR/ON measurement by Leuthold *et al.* (1980) on thermally prepared  $^{97}\text{RuFe}$  using the fast frequency sweep method gave a rough value for the SLR rate. A fast-cooling experiment (Murray *et al.* 1981) employing  $^{103}\text{RuFe}$  indicated a considerably higher rate. Later NMR/ON experiments used recoil-implanted samples as in the present work, but did not report values for the SLR rate (Eder *et al.* 1985). Here, we have applied the nonresonant TCON method to recoil-implanted samples in an effort to obtain reliable values of  $r_\infty$  for these two important cases.

## 2. Experiments

The experiments were performed using the TCON method, with a metallic weak thermal link between the sample and the mixing chamber of a dilution refrigerator (base temperature 4.5 mK). Details of the experimental setup and the data collection can be found in Beck (1997), Funk (1996) and Beck *et al.* (1998b). The samples were mounted together with a fast nuclear thermometer ( $^{54}\text{MnAg}$ ), permitting determination of the momentary lattice temperature,  $T_{\text{L}}(t)$ ; this is important in order to monitor the thermal response of the sample holder and to be able to extract accurate values of the SLR rate from the TCON data.

The relatively short-lived samples used in this work were top-loaded into the cold refrigerator soon after activation, which was performed at the ISL heavy-ion accelerator of the Hahn-Meitner-Institut in Berlin. The samples were prepared by recoil implantation of the radioactive impurity atoms following their production in heavy-ion reactions. This preparation method has the advantage that radiochemistry and thermal treatment of the starting material are avoided, and the overall impurity concentration (apart from impurities present in the

starting material) is kept low. We used 5N Fe foils of  $12.5 \mu\text{m}$  thickness as sample material. The  $^{57}\text{Ni}$  activity was produced in a fusion reaction between  $^{36}\text{Ar}$  and natural magnesium (mainly  $^{24}\text{Mg}$ ):  $^{24}\text{Mg}(^{36}\text{Ar}, n2p)^{57}\text{Ni}$ . The  $^{36}\text{Ar}$  beam had an energy of 105 MeV, slightly above the maximum in the reaction cross section. The  $1.5 \text{ mg/cm}^2$  Mg target foil was placed directly onto the Fe sample foil and held by a Ta collimator which defined the sample size. The beam, focussed to a circular spot of about  $1.5 \text{ mm}$  diameter, was swept vertically and horizontally at ca. 150 Hz within the  $5 \times 5 \text{ mm}$  collimator area during the irradiation to distribute the impurities evenly throughout the sample. The irradiation was carried out at about 400 nA beam current for 8 hours. The sample and target foils were mounted on a water-cooled target holder, but reached typically  $200^\circ\text{C}$  during the irradiation. The  $^{57}\text{Ni}$  produced (along with other isotopes from the same region of the nuclide table) recoils from the target foil with some tens of MeV energy and implants deeply (several  $\mu\text{m}$ ) into the sample material. Since  $^{57}\text{Ni}$  is far to the proton-rich side of the stability line, it must in any case be produced by a charged-particle reaction, and this method is the cleanest available for producing highly dilute *NiFe* samples.

The production of  $^{97}\text{RuFe}$  was similar, making use of the reaction  $^{61}\text{Ni}(^{40}\text{Ar}, \alpha)^{97}\text{Ru}$  using a  $1.9 \mu\text{m}$  target foil highly enriched in  $^{61}\text{Ni}$  and a beam of  $^{40}\text{Ar}$  at 130 MeV. Conditions were similar to those used in the *NiFe* preparation.

Recoil implantation (usually employing  $\alpha, xn$  reactions) has been used extensively for the preparation of samples for NMR/ON (see e.g. Eder *et al.* 1986; Ohya *et al.* 1985) as well as for in-beam PAD (e.g. Riegel and Gross 1988) and in-beam Mössbauer effect (Sielemann and Yoshida 1991), the last two making use of heavy-ion induced reactions. It is known from these extensive studies that the fraction of defect-associated impurities produced is quite small. Under the conditions of our irradiations, point defects anneal during the implantation. While recent experiments have indicated the formation of large fractions of interstitial impurity sites in some impurity-host combinations (Metz *et al.* 1993; Kapoor *et al.* 1997), these occur only when the impurity and the host are strongly 'mismatched' in atomic volume and electronegativity. The interstitial atoms are in any case not thermally stable, annealing under the implantation conditions used here. Our own experience with other 4d impurities in Fe prepared by heavy-ion induced recoil implantation (Brewer *et al.* 1994) has been encouraging. The two cases considered here, *NiFe* and *RuFe*, are characterised by high solubilities and by very similar atomic volumes and electronegativities of impurity atoms and host, so that the samples could, in principle, be prepared thermally. We are thus confident that a large fraction of the implanted impurities resides on substitutional, undisturbed sites in the Fe host lattice. This is confirmed by the observed  $\gamma$ -ray anisotropy in the case of  $^{97}\text{RuFe}$ .

High efficiency Ge detectors were mounted outside the cryostat for detection of  $\gamma$  rays (at  $0^\circ$  and  $90^\circ$  for the  $^{97}\text{RuFe}$  experiments, at  $90^\circ$  only for  $^{57}\text{NiFe}$ , since the  $\beta$  detector occupied the  $0^\circ$  radiation window; the angles are defined relative to the applied magnetic field, which was along the vertical cryostat axis, in the plane of the sample foils). In preliminary static nuclear orientation experiments, the  $\gamma$ -ray anisotropy as a function of temperature was measured and the half-life of the orienting parent state was redetermined. A check for thermal gradients between sample and thermometer was performed and any deviations of the

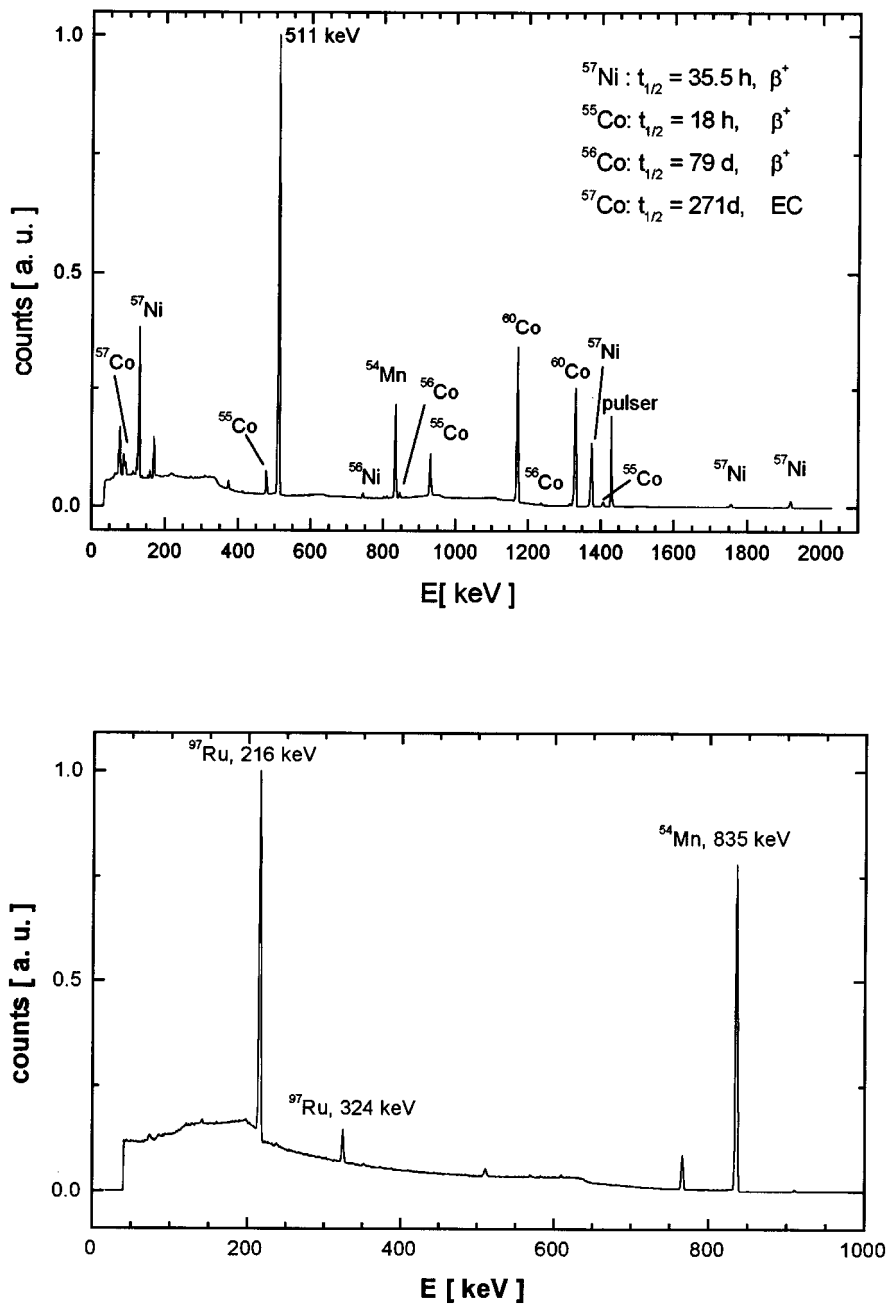


Fig. 1. Gamma-ray spectrum of a  $^{57}\text{NiFe}$  sample (upper part) about 4 h after completion of an implantation. Also seen are  $\gamma$ -ray lines from the  $^{54}\text{Mn}$  thermometry isotope and from  $^{60}\text{Co}$ , used for energy calibration. The lower part shows the gamma-ray spectrum of a  $^{97}\text{RuFe}$  sample, about 70 h after implantation. The 835 keV line from the  $^{54}\text{Mn}$  thermometry isotope is clearly seen.

observed anisotropy from the calculated values, which would indicate incomplete occupation of undisturbed sites by the impurity atoms, were investigated. Fig. 1 shows the  $\gamma$ -ray spectra of the two systems studied here, recorded some hours after the implantations.

For the reasons mentioned above, the  $\gamma$ -ray anisotropy signal from  $^{57}\text{NiFe}$  was too weak to be used for a TCON experiment. We therefore installed a  $\beta$ -particle detector in the cryostat to permit detection of the positrons emitted in the allowed (Gamow–Teller) decay of the  $I = \frac{3}{2}$  ground state of  $^{57}\text{Ni}$ . The detector consisted of a Si-based PIN diode (Hamamatsu S3590–06) mounted on the 4.2 K radiation window of the dilution cryostat beneath the sample. A 50  $\mu\text{m}$  thick Al window thermally attached to the 100 mK shield of the cryostat prevented an increased heat load to the sample due to thermal radiation from the detector. The diode was shielded by a copper collimator thermally anchored to the 4.2 K shield, with a 5 mm diameter circular opening defining the sensitive area for detection. Its cathode was electrically connected to the cryostat ground and its anode lead was passed out through the lower radiation windows of the cryostat using coaxial vacuum feedthroughs. A preamplifier (Ortec 142A) just outside the room-temperature window received and amplified the detector pulses. The detector was operated at a bias voltage of about 20 V. Its energy resolution was below 10 keV and it was found to be insensitive to the rf pulses used to heat the sample periodically in the TCON experiments. The background registered by the  $\beta$  detector due to electronic noise and natural background radiation was quite low in the energy windows used for the measurements (<100 counts per hour). The background from the  $^{54}\text{MnAg}$  nuclear thermometer (EC decay, one  $\gamma$ -ray at 835 keV) was measured in the standard experimental geometry and consisted mainly of the Compton distribution from the the single  $\gamma$  ray; it amounted to about 3% of the  $^{57}\text{Ni}$   $\beta^+$ -spectrum intensity at the beginning of an experiment. Energy calibration of the  $\beta$  detector was performed using the conversion electrons from a  $^{207}\text{Bi}$  source. Fig. 2 shows the pulse-height spectrum from the  $\beta$  detector with a  $^{57}\text{NiFe}$  sample and a  $^{54}\text{MnAg}$  thermometer mounted in the cryostat. The marked regions were used to evaluate the positron asymmetry and to carry out the TCON measurements. The low-energy shoulder is due to backscattered particles and was excluded from the signal region in the experiments. A lower threshold was set at about 150 keV to eliminate noise pulses (low energy cutoff in the figure). A precision pulser was used to check for drifts in the amplifier chain and to determine the deadtime in the pulse-height analysis system.

For the TCON experiments, heating pulses (using nonresonant rf power from a coil around the sample holder) were applied for a predetermined period during each time sweep; this was controlled by the computer which acquired the data. Gamma-ray and beta-particle spectra (usually with 1024 energy channels) were collected as a function of time (256 time channels, with heating during the first half of each sweep) to give 1024 x 256 counting-rate matrices. This procedure was repeated, with addition of the matrices, until sufficient counting statistics were obtained (usually, the sum matrix was stored after about one hour of counting, so that the data could be examined for temperature drifts and other instabilities before addition to give time-averaged data from a typical total measurement time of 12 hours.). Energy integration (with background subtraction for the  $\gamma$ -ray lines) was performed to reduce the amount of data in the spectra. In the case

of the  $\beta$ -particle spectra, integrations were first performed within the regions indicated in Fig. 2 ('region 1' and 'region 2') without background subtraction.

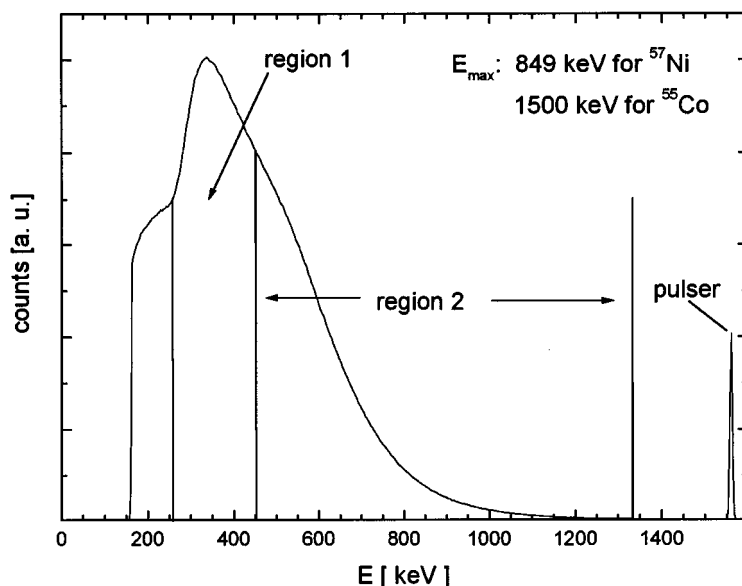


**Fig. 2.** Beta-particle spectrum obtained with the PIN diode from a  $^{57}\text{NiFe}$  sample with the  $^{54}\text{MnAg}$  thermometer in the experimental geometry. Energy regions 1 and 2 are indicated; the abscissa is in units of keV. The prominent shoulder near 200 keV is due to backscattered particles; the weak shoulder at 550 keV is the spectral maximum of the impurity isotope  $^{55}\text{Co}$ .

Background subtraction was then carried out separately for each region as a function of time to give counting rates (averaged over each time spectrum) which followed the exponential decay law for the known radioactive decay of  $^{57}\text{Ni}$ . [Its half-life was redetermined in a preliminary experiment using  $\gamma$ -ray spectroscopy and found to be  $1.479(8)$  days.] This procedure served to eliminate, to first order, background signals from contaminant isotopes (mainly  $^{55}\text{Co}$ ,  $^{56}\text{Co}$ ,  $^{56}\text{Ni}$  and  $^{57}\text{Co}$ ) also produced in the nuclear reaction used to prepare the samples. Of these,  $^{57}\text{Co}$  and  $^{56}\text{Ni}$  are of no consequence for the TCON measurement, since both decay by pure electron capture.  $^{56}\text{Ni}$  contributes only a constant (non-orienting) background due to its nuclear spin  $I = 0$ , and  $^{57}\text{Co}$  emits essentially only low-energy  $\gamma$  rays, below the regions of interest in the  $\beta^+$  spectrum. In addition, both were weak (relative activities at the beginning of a typical experiment compared to  $^{57}\text{Ni}$ : 2.1% and 1.85%, respectively). The comparatively long-lived (79 d)  $^{56}\text{Co}$  activity contributes a potentially troublesome temperature-dependent background to the  $\beta^+$  spectrum, but has a relative activity of only 0.5% at the beginning and 4.1% at the end of a typical experiment (ca. 100 h). The remaining important sources of background in the  $\beta^+$  spectrum are  $^{55}\text{Co}$  and the  $^{54}\text{Mn}$  used for thermometry. The former, due to its short half-life of 17.5 h and its strong  $\beta^+$  branching ratio, had a total activity about 70% of that of  $^{57}\text{Ni}$  at the beginning and 7.5% at the end of a typical experiment. The Compton distribution from the thermometer amounted to about 3% of the  $^{57}\text{Ni}$  beta intensity at the

beginning and about 25% at the end of an experiment. These contributions are removed to an accuracy level of 1% by the background subtraction procedure, but a temperature-dependent component might still remain, since they both show strong nuclear orientation under the conditions of the experiment. However, in the temperature range of these experiments, the change in count-rate expected for  $^{55}\text{CoFe}$  due to the thermal cycling is small ( $< 20\%$  of that seen for  $^{57}\text{NiFe}$ ) due to its relatively high interaction temperature  $T_{\text{int}} = 14.6$  mK and consequent saturation of its  $\beta^+$  asymmetry. Furthermore, both  $^{55}\text{CoFe}$  and  $^{54}\text{MnAg}$  exhibit much faster SLR rates than that found for  $^{57}\text{NiFe}$  (see below), and would tend to produce an artificial step in the measured relaxation curves at the beginning and end of each heating pulse. Since no such steps were observed (cf. Fig. 3), it can be concluded that these effects are small. If present, they would tend to simulate a higher SLR rate for  $\text{NiFe}$  than the true value. No background problems are encountered in the  $\gamma$ -ray spectra of  $^{97}\text{RuFe}$  (see Fig. 1). Here, the decay half-life was redetermined to be  $2.85(1)$  d.

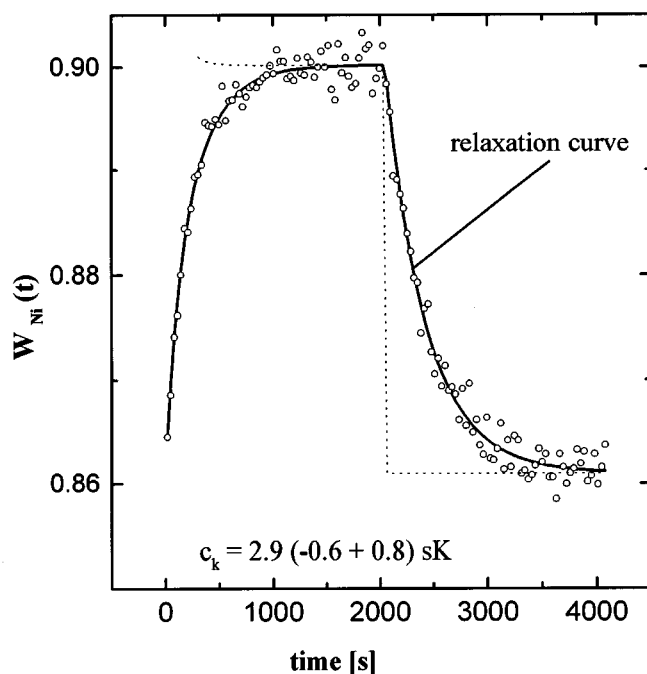


**Fig. 3.** Relaxation curve for  $^{57}\text{NiFe}$  (background corrected). The dotted curve indicates the lattice temperature  $T_L(t)$  as determined by the fast nuclear thermometer; it is essentially a step function on the time scale of the measurement. The solid curve is the fit to the multiexponential relaxation function taking the momentary temperatures into account.

On the time scale of the observed relaxation curve, the sample temperature in the  $^{57}\text{NiFe}$  experiments approximates the ideal case of a step function, cycling between the temperatures  $T_h = 9.8$  mK and  $T_l = 6.6$  mK. In the  $^{97}\text{RuFe}$  measurements, where the observed SLR rate is higher, some thermal hysteresis of the thermal link was observed (see Fig. 4), but it can readily be taken into

account in the fitting procedure for determining the relaxation constant  $C_{K\infty}$  from the relaxation curves. Again, a  $^{54}\text{MnAg}$  nuclear thermometer was used to determine curves of the lattice temperature  $T_L(t)$ , which could be used in the fitting process (cf. Fig. 4).

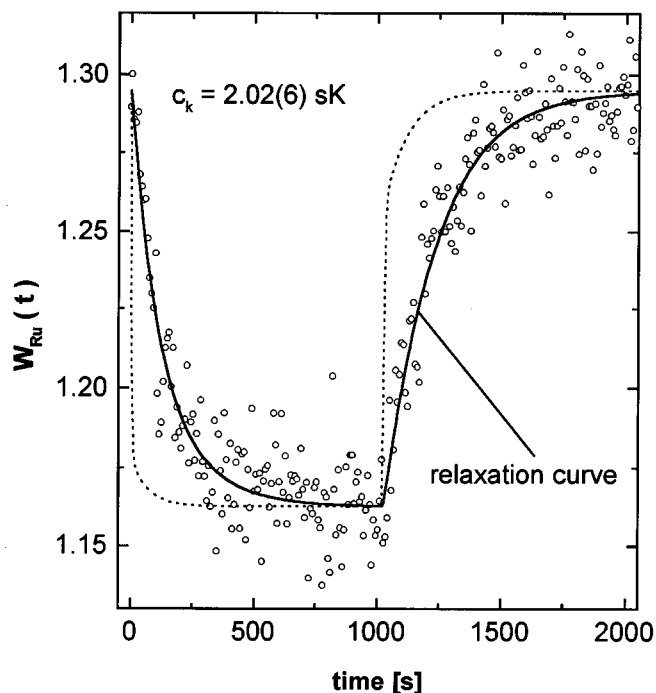


**Fig. 4.** Relaxation curve for  $^{97}\text{RuFe}$ , similar to Fig. 3. Here, the lattice temperature exhibits nearly a step function, and only a small 'tail' due to temperature-dependent heat capacities is present.

The multi-exponential relaxation function observed via the radiation anisotropy of oriented nuclei can be derived from the  $2I$  coupled rate equations which describe the nuclear relaxation at low temperatures (Bacon *et al.* 1972; Klein 1986). It is best computed numerically using an integration method such as the Runge-Kutta procedure, thus permitting the momentary lattice temperature  $T_L(t)$  to be taken into account at each step in the time spectrum (relaxation curve).

In the fitting process, the single relaxation constant  $C_K$ , which determines the time dependence of  $W(t)$ , is a free parameter. In addition, anisotropy parameters  $A_{\text{red}}$  and  $W_D$  ('anisotropy reduction' and 'drift' parameters), which allow for incomplete static orientation of the sample nuclei (see above) and for count-rate drifts during the experiment and have ideal values of 1.00, may also be left free when fitting the gamma-ray data. In the case of the positron asymmetry from  $^{57}\text{Ni}$ , the true asymmetry coefficient is in any case unknown, due to magnetic focussing and scattering of the  $\beta^+$  particles. These effects can again be collected into a reduction coefficient  $A_{\text{red},1}$  which multiplies the  $B_1$  term in the expression for the beta asymmetry. Including also the energy-dependent

asymmetry reduction  $v/c$  due to the fact that the emitted positrons are not completely relativistic, we find that  $v/c A_{\text{red},1}$  was about 0.16 in the lower energy region (region 1 in Fig. 2) and 0.25 in the upper region. This reduction in signal is more than compensated by the large increase in count-rate (a factor of about 17 at  $B_0 = 1.25$  T) provided by the focussing of practically all the beta particles emitted towards the lower hemisphere into the detector. The actual value of the reduction factor has essentially no influence on the final result for  $C_K$ . The temperature versus time curve,  $T_L(t)$ , is obtained from the thermometer data. Observed variations in the fitted value of  $C_K$  with variations of the temperature within the statistical accuracy of the thermometry and, in the case of  $^{57}\text{NiFe}$ , with the energy region chosen in the beta spectrum and the background correction (data from different times during an experiment) were used to estimate the uncertainties in the reported  $C_K$  values. These variations are generally considerably larger than the fit errors alone, which underestimate the true experimental uncertainties. More details of the measurement procedure and the data analysis can be found in Beck (1997).

**Table 1. Relaxation rates for NiFe and RuFe**

Isotope	Half-life (days) <sup>A</sup>	Nuclear spin $I$	Magnetic moment ( $\mu_N$ )	$T_l$ (mK)	$T_h$ (mK)	Static hyper- fine field $B_{\text{hf}}$ (T)	$C_{K\infty}$ (sK)	$r_\infty$ ( $10^{-15}$ $\text{T}^2 \text{ s K}^{-1}$ )
$^{57}\text{Ni}$	1.479(8)	$\frac{3}{2}$	0.792(8)	6.6	9.8	-23.4(1)	2.94( $^{+0.69}_{-0.64}$ )	0.54( $^{+0.14}_{-0.11}$ )
$^{97}\text{Ru}$	2.85(1)	$\frac{5}{2}$	0.787(8)	5.2	8.5	-48.96(40)	2.02(6)	2.17(6)

<sup>A</sup>Values redetermined in this work.

### 3. Results and Discussion

The relaxation constants  $C_{K\infty}$  (i.e. the high-field limiting or intrinsic values) for extremely dilute NiFe and RuFe were determined using the procedures outlined above to be 2.9 ( $-0.6/+0.7$ ) sK for  $^{57}\text{NiFe}$  and 2.02 (6) sK for  $^{97}\text{RuFe}$ . The corresponding isotope-independent relaxation rates  $r_\infty$ , defined as  $r_\infty = (\gamma^2 C_{K\infty})^{-1}$ , are given in Table 1 (in the usual units of  $10^{-15}$  sT<sup>2</sup>/K), along with the parameters used in the data analysis. We note that due to the relatively short half-lives of the isotopes used here, no attempt was made to study the field dependence of  $C_K$ ; instead, in the interest of a more precise determination of the intrinsic relaxation constants  $C_{K\infty}$ , measurements were made at a single applied field of 1.25 T, which is known from a large number of other cases to correspond to saturation of the field dependence, i.e. to the intrinsic relaxation rate.

As mentioned above, there has been one previous estimate of the relaxation rate of NiFe, based on the FM-on/off method using NMR/ON (Ohtsubo *et al.* 1996). In this method, the initial state for relaxation depends on the degree of resonance saturation reached under the given experimental conditions and is not, in general, well-defined (although the use of a source term in the rate equations accompanied by a systematic study of resonance saturation seems to give reliable values for the relaxation constants; see e.g. Hagn and Zech 1984). An additional difficulty with the SLR rate as determined by Ohtsubo *et al.* (1996)

is that they carried out the measurement at an applied field of only 0.2 T and fit the relaxation curves with a simple exponential function. The latter point may not be serious, since for the orientation parameter  $B_1$  which governs the observed  $\beta$ -particle asymmetry, the quoted measurement temperature of 8 mK, corresponding to  $T_L/T_{\text{int}} = 1.8$ , is not too far from the high-temperature limit (see Klein 1986), where in fact  $B_1$  *does* relax following a single exponential function with a time constant corresponding to  $C_K$ . The good fit obtained by Ohtsubo *et al.* (1996) is indicative of this fact. A rough estimate shows that the second exponential term in the multi-exponential relaxation function is about a factor of 20 smaller than the main term, and the third term is negligible; thus the single-exponential approximation is not too bad, although the quoted (fit) error certainly still underestimates the uncertainty in the resulting  $C_K$  value. More serious is the low measurement field. The applied field dependence of  $C_K$  has not been determined for  $\text{NiFe}$ , and in any case the amplitude of the increase in relaxation rate on going from the high-field limit to low fields appears to be sample dependent (cf. Bobek *et al.* 1993). An estimate based on the neighbouring  $\text{CoFe}$  system would indicate that  $C_{K\infty}$  should be about a factor of 1.5 larger than the value of  $C_K$  measured at  $B_0 = 0.2$  T. Using the reported time constant of 260(10) s at 8 mK and the above estimate for the applied field correction, we derive from Ohtsubo *et al.* (1996) a value of  $C_{K\infty} = 3.12(12)$  sK for the intrinsic relaxation constant of  $^{57}\text{NiFe}$  (fit error only). This agrees very well with our result, although the good agreement is probably fortuitous, given the uncertainties in the recalculation.

For the case of  $\text{RuFe}$ , two previous estimates of the SLR rate are available. The value 1.7 sK (Leuthold *et al.* 1980, recalculated by Klein 1986) from a nuclear resonance experiment on  $^{97}\text{Ru}$  in a ca. 1%  $\text{RuFe}$  alloy (prepared by thermal alloying and reactor irradiation) is in reasonable agreement with our result. The much faster relaxation reported by Murray *et al.* (1981), who applied the fast cooling method to dilute  $^{103}\text{RuFe}$ , would seem to be in error, since it gives a relaxation rate more than twice that of the present work and of Leuthold *et al.* (1980). This high value also falls well outside the systematics for other 4d impurities in Fe (cf. Fig. 5).

In Fig. 5, we show the reduced relaxation rates  $r_\infty$  for 3d and 4d impurities in Fe, plotted along each series as a function of impurity  $Z$ . The calculated rates of Akai (1988) are also shown, along with phenomenological estimates of the additional contribution due to VSW excitation (Weger 1962; Masuda *et al.* 1974).

The values reported here for  $r_\infty$  of  $\text{NiFe}$  and  $\text{RuFe}$  nearly complete the systematics for these two series of impurities in an Fe host. It may be seen that the calculations of Akai as published give SLR rates  $r_\infty$  which are in reasonably good agreement with the experimental rates in the 3d series. Discrepancies still exist for Mn and Co impurities which are well outside the experimental uncertainties. The present value for  $\text{NiFe}$  is in reasonably good agreement with the predicted rate; we note that it is one of the very few cases where the experimental rate is *smaller* than the calculated one. (In this connection it is interesting that correction for all of the systematic errors likely to be present in our value would reduce the rate still further.) Addition of the relaxation rates due to the VSW mechanism generally worsens the agreement for this series, although they are

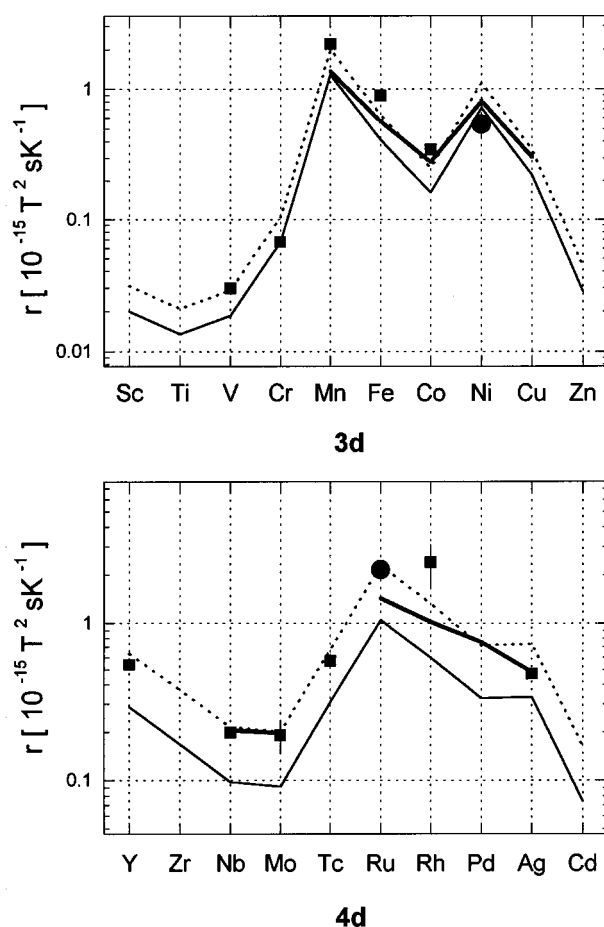


**Fig. 5.** Overall systematics (intrinsic SLR rates  $r_{\infty}$  versus impurity  $Z$ ) for dilute 3d series (upper diagram) and 4d series (lower diagram) impurities in an Fe host. The data points reported in this work are shown as circles. Other data (squares) for the 3d series are (for Fe) from Ohtsubo *et al.* (1996); for V, Cr and Mn from Boysen *et al.* (1984); and for Co from Kopp *et al.* (1981). In the 4d series, the Y datum is from Fahad *et al.* (1988), the Nb and Tc data are from Brewer *et al.* (1994), the Mo datum from Hagn and Zech (1984), and the Rh and Ag points were taken from the compilation in Klein (1986). The full curves represent the calculations of Akai (1988), the dashed curves are Akai's results scaled upwards by a factor of 1.5 (3d series) or 2.2 (4d series), and the thick full curve is the sum of Akai's values and an estimated virtual spin-wave contribution (cf. Masuda *et al.* 1974).

small and the changes are not significant. In the 4d series, on the other hand, the agreement with the calculated rates is generally poorer (the experimental rates are underestimated by nearly 100% in all cases), but inclusion of the (larger) estimated VSW-mechanism rates gives much better agreement. However, simply scaling the calculated values by a factor of 2.2 gives an equally good improvement in agreement (compare also the 5d series, Beck *et al.* 1998a).

Experimentally, determination of the SLR rates for dilute  $\text{ScFe}$ ,  $\text{CuFe}$ ,  $\text{ZrFe}$  and  $\text{PdFe}$ , as well as a new determination for  $\text{RhFe}$ , would make a clearer

comparison with theory possible. It is also apparent that new calculations are needed and that the Weger mechanism may play an important role in explaining the observed relaxation rates.

### Acknowledgments

We wish to thank Mr J. Thiel for assistance with the apparatus. Our samples were irradiated at the ISL accelerator of the Hahn-Meitner-Institut Berlin, and we thank the ISL staff as well as Dr P. West of the FU Berlin. Professor P. Herzog, Bonn, provided very helpful information on the diodes we used as beta-particle detectors.

### References

- Akai, H. (1988). *Hyp. Interact.* **43**, 255.
- Akai, H., Akai, M., Blügel, S., Drittler, B., Ebert, H., Terakura, K., Zeller, R., and Dederichs, P. H. (1990). *Prog. Theor. Phys. Suppl.* **101**, 11.
- Bacon, F., Barclay, J. A., Brewer, W. D., Shirley, D. A., and Templeton, J. E. (1972). *Phys. Rev. B* **5**, 2397.
- Beck, E. (1997). Kernspin-Gitter-Relaxation von d-Elementen in Fe und Co. PhD Dissertation, F.U. Berlin (unpublished).
- Beck, E., Brewer, W. D., Funk, T., Bobek, C., and Klein, E. (1998a). *Aust. J. Phys.* **51**, 281.
- Beck, E., Brewer, W. D., Funk, T., Bobek, C., and Klein, E. (1998b). Systematics of the nuclear spin-lattice relaxation of transition-element impurities in Fe. *J. Mag. Mag. Mater.*, submitted.
- Bobek, C., Dullenbacher, R., and Klein, E. (1993). *Hyp. Interact.* **77**, 327.
- Boysen, J., Brewer, W. D., Bures, K.-D., Kettschau, A., Klein, E., Kopp, M., and Wilson, G. V. H. (1984). *J. Mag. Magn. Mat.* **43**, 267.
- Brewer, W. D., Hobuß, U., Metz, A., and Riegel, D. (1994). *Physica B* **194-96**, 359.
- Eder, R., Hagn, E., and Zech, E. (1985). *Phys. Rev. C* **32**, 1707.
- Eder, R., Hagn, E., and Zech, E. (1986). *Nucl. Phys. A* **451**, 46.
- Fahad, M., Berkes, I., Hassani, R., Massaq, M., Shaw, T. L., and Stone, N. J. (1988). *Hyp. Interact.* **43**, 307.
- Funk, T. (1996). Kernspin-Gitter-Relaxation von Osmium in Eisen. Master's Thesis (Diplom), F.U. Berlin (unpublished).
- Hagn, E., and Zech, E. (1984). *Phys. Lett. A* **101**, 49.
- Kapoor, J., Riegel, D., Yi Li, Polaczyk, C., Andres, J., Mezei, F., Sielemann, R., Yoshida, Y., Brewer, W. D., de Mello, L. A., and Frota-Pessôa, S. (1997). *Phys. Rev. Lett.* **78**, 1279.
- Klein, E. (1986). In 'Low Temperature Nuclear Orientation' (Eds N. J. Stone and H. Postma), Ch. 12 (North Holland: Amsterdam).
- Kopp, M., Kazemi-Far, B., and Klein, E. (1981). *Z. Phys. B* **44**, 73.
- Leuthold, K., Hagn, E., Ernst, H., and Zech, E. (1980). *Phys. Rev. C* **21**, 258.
- Masuda, Y., Hioki, T., and Kontani, M. (1974). *Int. J. Magnetism* **6**, 143.
- Metz, A., Frota-Pessôa, S., Kapoor, J., Riegel, D., Brewer, W. D., and Zeller, R. (1993). *Phys. Rev. Lett.* **71**, 3525.
- Murray, D. W., Allsop, A. L., and Stone, N. J. (1981). *Hyp. Interact.* **11**, 127.
- Ohya, S., Nishimura, K., and Mutsuro, N. (1985). *Nucl. Phys. A* **445**, 29.
- Ohtsubo, T., Cho, D. J., Yanagihashi, Y., Komatsuzaki, K., Mizushima, K., Muto, A., and Ohya, S. (1996). *Hyp. Interact. C* **1**, 577.
- Riegel, D., and Gross, K.-D. (1988). In 'Nuclear Physics Applications on Material Science' (Eds E. Recknagel and J. C. Soares), Vol. 144, p. 327 (NATO-ASI Series E).
- Rosenblum, S. S., and Steyert, W. A. (1975). *Phys. Lett. A* **53**, 34.
- Seewald, G., Hagn, E., and Zech, E. (1997). *Phys. Rev. Lett.* **78**, 5002.
- Sielemann, R., and Yoshida, Y. (1991). *Hyp. Interact.* **68**, 119.
- Weger, M. (1962). *Phys. Rev.* **128**, 1505.